Research article

Heart rate detection method based on Ballistocardiogram signal of wearable device : Algorithm development and validation

Duyan Geng [a,b], Yue Yin [a,b], Zhigang Fu [c], Geng Pang [a,b], Guizhi Xu [a,b], Yan Geng [d,*], Alan Wang [e,f]

[a] Hebei University of Technology, State Key Laboratory of Reliability and Intelligence of Electrical Equipment, Tianjin, 300130, PR China
[b] Hebei University of Technology, School of Electrical Engineering, Tianjin, 300130, PR China
[c] Physical Examination Center of the Fourth Joint Logistics Support Unit of the 983rd Hospital of the Tianjin Chinese People's Liberation Army, Tianjin, 300142, PR China
[d] Hebei Institute for Drug and Medical Device Control, Shijiazhuang, 050200, PR China
[e] Centre for Brain Research, Faculty of Medical and Health Sciences, University of Auckland, Auckland, New Zealand
[f] Centre for Medical Imaging, Faculty of Medical and Health Sciences, University of Auckland, Auckland, New Zealand

ARTICLE INFO

ABSTRACT

Background: Heart rate, as the four vital signs of human body, is a basic indicator to measure a person's health status. Traditional electrocardiography (ECG) measurement, which is routinely monitored, requires subjects to wear lead electrodes frequently, which undoubtedly places great restrictions on participants' activities during the normal test. At present, the boom of wearable devices has created hope for non-invasive, simple operation and low-cost daily heart rate monitoring, among them, Ballistocardiogram signal (BCG) is an effective heart rate measurement method, but in the actual acquisition process, the robustness of non-invasive vital sign collection is limited. Therefore, it is necessary to develop a method to improve the robustness of heart rate monitoring.

Objective: Therefore, in view of the problem that the accuracy of untethered monitoring heart rate is not high, we propose a method aimed at detecting the heartbeat cycle based on BCG to accurately obtain the beat-to-beat heart rate in the sleep state.

Methods: In this study, we implement an innovative J-wave detection algorithm based on BCG signals. By collecting BCG signals recorded by 28 healthy subjects in different sleeping positions, after preprocessing, the data feature set is formed according to the clustering of morphological features in the heartbeat interval. Finally, a J-wave recognition model is constructed based on bi-directional long short-term memory (BiLSTM), and then the number of J-waves in the input sequence is counted to realize real-time detection of heartbeat. The performance of the proposed heartbeat detection scheme is cross-verified, and the proposed method is compared with the previous wearable device algorithm.

Results: The accuracy of J wave recognition in BCG signal is 99.67%, and the deviation rate of heart rate detection is only 0.27%, which has higher accuracy than previous wearable device algorithms. To assess consistency between method results and heart rates obtained by the ECG, seven subjects are compared using Bland-Altman plots, which show no significant difference between BCG and ECG results for heartbeat cycles.

---

* Corresponding author.
E-mail address: ygeng102588@sina.com (Y. Geng).

Conclusions: Compared with other studies, the proposed method is more accurate in J-wave recognition, which improves the accuracy and generalization ability of BCG-based continuous heartbeat cycle extraction, and provides preliminary support for wearable-based untethered daily monitoring.

1. Introduction

With the progress of society and the continuous improvement of people's living standards, the high intensity of mental and physical work makes health become the focus of people's attention. Heart rate, as the four vital signs of human body, is a basic indicator to measure a person's health status [1,2]. Heartbeat detection and analysis can effectively evaluate sympathetic and parasympathetic nerve activity state of subjects, so as to deduce the emotional change, stress level, sleep quality, and other physical and psychological condition information [3]. This has positive implications for the health and care of the subjects. Traditional heartbeat detection based on ECG has the advantages of obvious signal characteristics, easy detection, simple algorithm and high detection accuracy. However, due to the fact that ECG signal is directly collected from the subjects, it is necessary to always wear lead electrodes, which undoubtedly poses significant limitations on the activities of normal participants during the testing process [4]. In contrast, Ballistocardiogram (BCG)-assisted heart rate monitoring has garnered considerable attention in both academia and industry due to its non-invasive, simple, and cost-effective nature. BCG system generally uses piezoelectric, acceleration and other non-contact sensors to capture the impact force of blood-on-blood vessels in each heartbeat. These sensors can be placed under the seat [5] in daily work, under the pillow [6] in the bedroom, and on the bed [7], etc., to collect signals without affecting the daily life of the subject.

Nowadays, many medical detection systems need to process a large number of physical signals, including BCG signals and ECG signals. However, it is particularly important to better process these signals and extract data that is conducive to our analysis [8]. proposes a good detection method for hypertension and its complications, which is based on machine learning and signal processing methods to accurately classify patients' ECG signals [9]. focuses on the challenge of hypertension management, which, if not regulated, can lead to serious complications such as stroke and heart disease. Therefore, the author adopts the continuous wavelet transform method to transform the BCG signal, thereby achieving the training of the 2D convolutional neural network model (2D-CNN) and ensuring high accuracy. Based on this [10], further reviews physiological signals that can be used for health monitoring, such as ECG, BCG, and HRV. This further proves the effectiveness of machine learning methods and deep learning methods based on ECG or BCG signals, providing a foundation for the development of wearable devices [11]. proposes a combination of empirical mode decomposition and wavelet transform to identify hypertension based on BCG signals. The highest average classification accuracy can be achieved at 89% [12]. used the k-nearest neighbor, support vector machine, and ensemble bagged trees classifiers to classify hypertension, and their high accuracy can meet the requirements of remote hypertension monitoring based on ECG signals [13]. mentions that early monitoring can effectively prevent various cardiovascular diseases caused by hypertension. The proposed method can be effectively applied to intensive care units, which is beneficial for screening electrocardiogram signals while monitoring sudden increases in blood pressure. Therefore, both ECG and BCG signals are effective data for analyzing health status.

BCG signal is used to reflect the beating characteristics of the heart because it is derived from the signals generated by beating, and this mechanical signal is used to show the pumping process of the heart, such as changes in body surface displacement [14]. A typical BCG signal often contains a 'W' shaped wave group which is complex formed by H, I, J, K, and L [15]. The BCG signal and the ECG signal are correlated, which is reflected in the J wave and the R wave. Whether the J-wave positioning is accurate means that the maximum amplitude point of the heartbeat cycle is monitored normally, and represents the core of heartbeat detection [16]. At present, the commonly used J-wave localization methods include template matching method, differential threshold method, and unsupervised learning method. Shin [17] used the template matching method to collect the I-J-K complexes of BCG to build a template library, and realized template matching through a local moving window, and detected heartbeats according to the correlation coefficient. Will, C [18] made a template matching into the cross-correlation method, which improves the detection accuracy. Regarding the threshold method and its improved algorithm, Jingjing Jin [19] used adaptive threshold wavelet contractions to preprocess BCG and then detected the subject's heart rate through pseudo-cycle detection; Ren Yu [20] used the monitoring method of the maximum difference between adjacent peaks and troughs to calculate the heartbeat. This method did not rely on the heartbeat template, and directly detected the heartbeat through BCG beat. Brüser [21] calculated the peak group features of BCG signals, and used an unsupervised learning clustering algorithm to distinguish J waves from other peaks; Shen [22] extracted the peak features of BCG signals, and used mixture Gaussian model clustering and correlation coefficient filtering to determine J waves, wave position, and then calculated the beat interval.

Due to the change of amplitude and distance of each wave crest, the waveform is no longer obvious in the acquisition process [23]. Therefore, the above heartbeat detection methods have a strong dependence on morphological standards and single-mode BCG signals. The characteristics of BCG is the key to solving such problems. In recent years, due to the popularity of deep learning, in the face of large and complex data, neural network can automatically read useful information from the data without prior knowledge, thereby effectively training recognition model. Both ECG and BCG are time-series signals, which represent a large number of regular time-series features during the periodic beating of the heart. Bi-directional Long Short Term Memory (BiLSTM) has the inherent advantage of extracting correlation features from time series. Heart rate information has temporal characteristics, and this advantage is widely used in the research of heart rate recognition [24], and Oliver [25] used LSTM networks to identify and predict atrial fibrillation [26]. used a BiLSTM network to decompose the ECG signal by wavelet as the first layer input of the model, which improved the

accuracy of five types of heart rate recognition. Fotiadou [27] used convolutional neural networks (CNN) combined with LSTM networks to capture the short- and long-term temporal dynamics of fetal heart rate, and achieved good recognition results on datasets recorded during labor. Many studies have shown that LSTM can be effectively used in time series signals and can record long-term feature information in time series data.

In this study, in view of the advantages of sequence processing network processing such as LSTM in effectively extracting and predicting time series features, we propose a heartbeat detection method based on BiLSTM for accurate localization of J wave of BCG signals, which has high robustness and generalization ability for cardiac shock signals under different sleeping postures. By extracting the peak feature parameters in BCG, we establish the labeled feature set. Secondly, BiLSTM uses the input of BCG signal to mine the timing characteristics, and then realizes the identification and classification of BCG signal peaks. The classification accuracy is validated using a multi-recognition model, and the heart rate calculation method's effectiveness is verified by comparing the classification results with real labels.

2. Dataset

2.1. Data collection

A group of 16 women and 12 men, randomly distributed between the ages of 18 and 50, were recruited to meet the needs of the experiment. Recruitment and inclusion criteria: 1) Not diagnosed with heart-related diseases by medical institutions; 2) Healthy limbs and no mental illness; 3) Informed and consented to the content of this experiment, and all participants are voluntary. This experiment adheres to the ethical principles of the Declaration of Helsinki, and the experiment is conducted after volunteers have read the purpose and procedure of the experiment in detail and signed an informed consent form.

The BCG signal acquisition equipment adopts DEEBCG pillow (Zhejiang Deyi Software Technology Co., Ltd., China). DEEBCG can detect BCG, breathing, and other body movements. The measurement initiates automatically shortly after the user retires to bed and ceases recording upon their departure from the bed in the morning. Processed BCG signals are transmitted to the cloud from the device, enabling users to access corresponding data effortlessly on the client side. This approach is contact-free, requiring minimal effort from the user, and promotes daily compliance by enhancing user-friendliness.

The three-lead ECG acquisition system is used to acquire reference signals, that is, the subjects are connected to the acquisition system at the same time to ensure the synchronization of signal acquisition and reduce signal interference, which is conducive to improving the accuracy of the acquisition process and convenient for the experimentalists to collect signals. The original ECG signal is amplified, filtered and level raised, digital-to-analog conversion is performed by MS430 single-chip microcomputer, and the sampling frequency is set to 1000Hz. Finally, the data is uploaded to the host computer through the Bluetooth module for storage and analysis. The Pan-Tumpkins algorithm is used to detect R the waves in ECG and the RR interval is extracted, and the data is used as the standard reference data.

The data collection process is shown in Fig. 1. The DEEBCG pillow is placed under the pillow, and the subject is connected to the ECG system and lay on the bed. Participants naturally relax on the bed to rest. The 4 sleeping positions of prone, supine and left and right are collected for 10 min each.

2.2. Data labeling

In this paper, the BiLSTM deep learning algorithm is used for J-wave positioning, and the data is input in the form of sequence
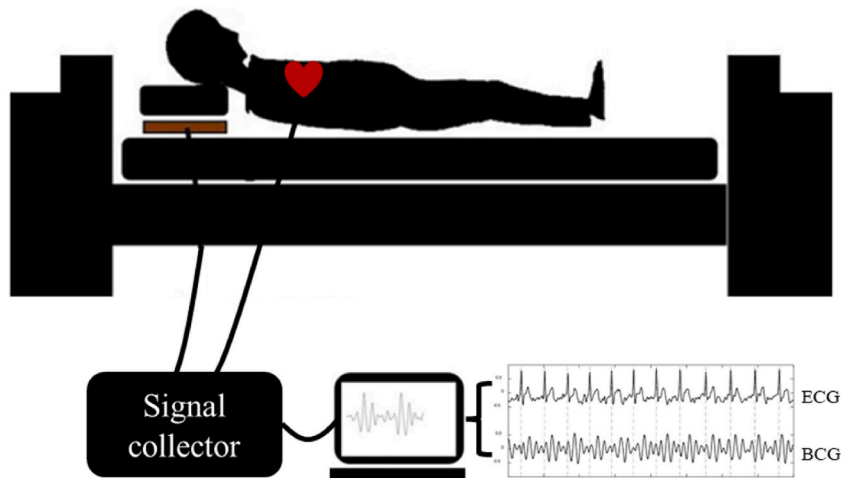

Fig. 1. Schematic diagram of BCG and ECG synchronous acquisition system.

fragments. Therefore, the collected data needs to be labeled and processed in segments. All BCG data are detected by sliding window threshold [28]. Because BCG signal is easily affected by motion vibration, the amplitude of motion artifact is much higher than that of BCG signal. If the signal amplitude is not within the normal threshold, the BCG signal of stationary segment will be removed and divided by manual screening. Considering that the BCG signal will be affected by different sleeping positions, the "W" complex of the BCG signal will be different, and neither the threshold method nor the template method is applicable to the dataset of this study. The core of clustering method is the subset division. The similarity within these disjoint sets is greater than that outside the set, and the similarity between different sets can be lower through certain rule division. Therefore, the clustering method is used to identify and classify the crest of BCG signal, and there is a certain periodicity in J-point positioning. The specific steps are as follows:.

(1) Retrieve the k sampling points of the signal S in the interval, and find out all the peaks and valleys of the signal S and the corresponding index positions, as shown in equations (1) and (2):

$$\left| \begin{cases} | \ \text{Pamp}(k) = S(k) \\ | \ \text{Ppos}(k) = k \end{cases} \right.$$
$$| \ S(k) > S(k-1) \cap S(k) > S(k+1) \tag{1}$$

$$\left| \begin{cases} \text{Tamp}(k) = S(k) \\ | \ \text{Tpos}(k) = k \end{cases} \right.$$
$$| \ S(k) < S(k-1) \cap S(k) < S(k+1) \tag{2}$$

Among them, P_{amp} represents the peak amplitude, P_{pos} represents the peak index, T_{amp} represents the trough amplitude, and T_{pos} represents the trough index.

(2) As shown in Fig. 2, using all the peak trough and peak information for parameter calculation, calculate 4 parameters for each crest, respectively, the amplitude Pa(n) of the peak P(n), the amplitude of the peak T(n) adjacent to the trough T(n) Ta(n), the distance between the peak P(n) and the trough T(n) is Pd(n), the distance between the T(n) and the P(n+1) is Td(n), and the parameter expressions are shown in equations (3)–(6):

$$Pa(n) = Pamp(n) \tag{3}$$

$$Ta(n) = Tamp(n) \tag{4}$$

$$Pd(n) = Tpos(n) - Ppos(n) \tag{5}$$

$$Td(n) = Ppos(n+1) - Tpos(n) \tag{6}$$

Construct a feature set, and consider 5 consecutive peaks in the feature set. Each feature vector has a dimension of 20, including parameters of each peak, as shown in the following formula:
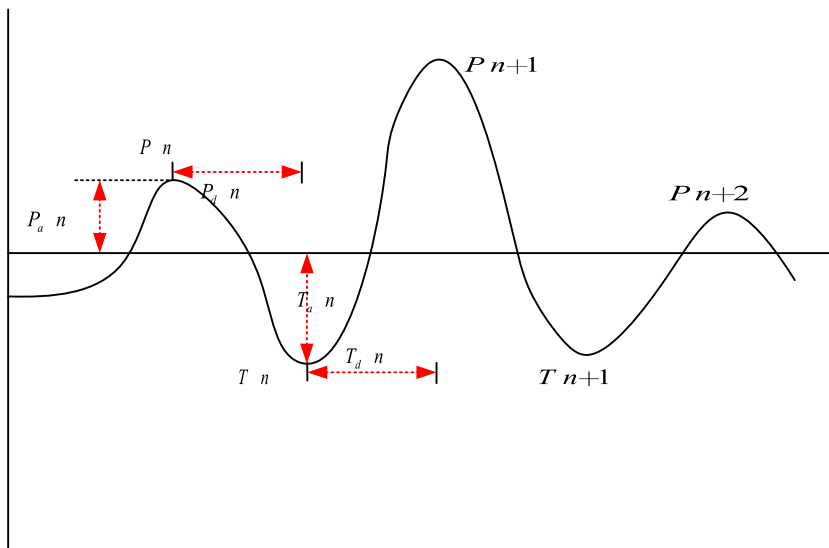

Fig. 2. Characteristic parameters of wave peaks and troughs.

$$f_n(Pa(n), Ta(n), Pd(n), Td(n), \ldots, Pa(n+4), Ta(n+4), Pd(n+4), Td(n4)) \tag{7}$$

(3) The number of clusters is set to 5, and the Euclidean distance is used as the reference basis to achieve the best arrangement of the feature set, which is conducive to indexing.

After K-means clustering distinguishes each wave crest, to ensure the accuracy of sample space construction, perform the following operations:

1) In this experiment, the J wave has more obvious morphological characteristics than other peaks, and the clustering effect is the best. Therefore, the J wave is used as the benchmark to compare the synchronously collected ECG signals for manual verification. The verification criteria encompass confirming whether the J wave is situated between two adjacent R waves, ensuring the consistency between the count of J waves and R waves, and validating whether the positions of the J waves, H, and I waves adhere to the characteristics of the BCG signal. According to the verification standard, each piece of data is reviewed by another person after verification, and a total of 3 times is reviewed to ensure the accuracy of the J-wave marking. After review, according to the peak index of each wave, the J wave that cannot be successfully identified or identified by the k-means clustering algorithm is corrected, so as to ensure the quality of the dataset.
2) According to the J-wave position after the above review, locate the positions of the H wave and the L wave respectively. In order to make the classification of the samples in the dataset balanced, the J wave in each BCG signal is marked as 1, the H wave is marked as 2, the L wave is marked as 3, and the rest of the peaks are marked as 0. An example of the labeling result is shown in Fig. 3.
3) Sequence segmentation was performed on the collected BCG signal data, and sequences with less than 100 peaks were removed to construct the feature set. The dataset eventually contained 1190 heartbeat sequences, for a total of 19,375 heartbeats.

3. Model building

3.1. Model training

BiLSTM uses recurrent neural network to achieve forward recursion and reverse recursion, and the specific structure is shown in Fig. 5. LSTM has strong learning ability for long-term dependent information. Input gate, output gate and forget gate are the three necessary units. In order to solve the problem of disappearing gradient, the current state is used to control the output result [29]. The information stored in the original cells is transmitted to the system through the forget gate to activate the normal operation of each cell. The forget gate expression is shown in formula (8):

$$\Gamma_f = \sigma\left(w_f\left[h^{(t-1)}, x^{(t)}\right] + b_f\right) \tag{8}$$

Among them, σ is the sigmoid activation function, w_f is the forgetting gate weight matrix, $h^{(t-1)}$ is the hidden layer state at (t-1) time, $x^{(t)}$ is the input at time t, and b_f is the forgetting gate intercept.

Next, The input gate expression and the cell state correction value expression are respectively shown in equations (9) and (10):

$$\Gamma_i = \sigma\left(w_i\left[h^{(t-1)}, x^{(t)}\right] + b_i\right) \tag{9}$$

$$\widetilde{C^{(t)}} = \tan h\left(w_c\left[h^{(t-1)}, x^{(t)}\right] + b_c\right) \tag{10}$$

Among them, w_i, b_i is the input gate weight and intercept, w_c, b_c is the cell state correction weight and intercept.

Finally, the expression of the output gate, the expression of the current cell state and the expression of the hidden layer at the current moment are shown in equations (11)–(13):

$$\Gamma_o = \sigma\left(w_o\left[h^{(t-1)}, x^{(t)}\right] + b_o\right) \tag{11}$$

$$C^{(t)} = \Gamma_i * \widetilde{C^{(t)}} + \Gamma_f * C^{(t-1)} \tag{12}$$
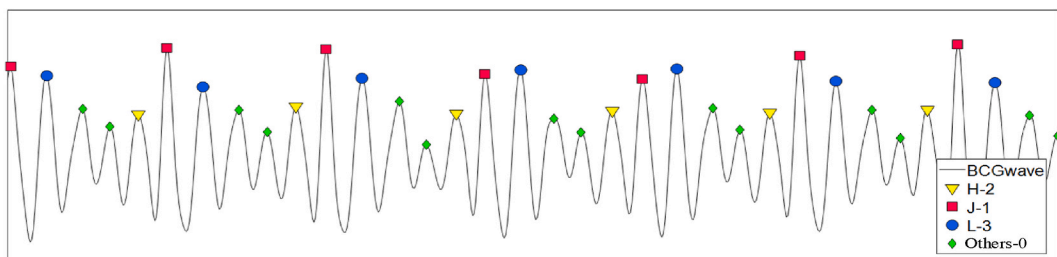

Fig. 3. Example of a peak marker.

$$h^{(t)} = \Gamma_o * \tan hC^{(t)} \tag{13}$$

Among them, w_o, b_o is the output gate weight and intercept, and tanh is the hyperbolic tangent function.

Compared with LSTM, which can only predict the forward sequence, the forward activation function and backward activation function of BiLSTM can be predicted simultaneously, and the forward and reverse sequence information can be captured at the same time. For the BCG cardiac peak group sequence in this paper, BiLSTM can combine the peak information before and after a certain time to make the sequence features of the target peaks in the peak group more prominent. Therefore, this paper uses BiLSTM to intelligently identify the BCG continuous peak sequence features. As shown in Fig. 4, the output mode of the BiLSTM model used in this paper is a many-to-many mode, each sequence data contains 100 steps, and the output produces 100 classification results.

Fig. 5 shows the designed system architecture. It adopts the structure design of 1 input layer, 2 hidden layers (composed of BiLSTM) and 1 output layer. The input layer adopts the marked feature set, and the dimension 100*3.100 is the time collection point, that is, the wave crest information. 3 is the parameter, that is, the characteristic parameter of each wave crest information. These features together form the feature set, including the distance between two adjacent peaks and the amplitude of each crest. In terms of hidden layer settings, in order to take into account the training effect and efficiency, after many experiments, two layers of BiLSTM layers and two layers of fully connected layers are used. The primary role of the fully connected layer is to flatten the multi-dimensional sequence output into a feature vector, and then map these distributed features to the sample label space. The initial BiLSTM layer comprises 128 hidden layer units, while the subsequent BiLSTM layer consists of 64 hidden layer units. Both fully connected layers are configured with 32 and 16 hidden layer units respectively, employing the rectified linear unit (ReLU) activation function. For the output layer, the softmax activation function is utilized to execute logistic regression for classifying the four output results. The network optimization strategy employs the adaptive moment (Adam) optimizer, with the cross-entropy loss function utilized as the loss function [30]. Following each iteration, the network connection weights and biases are adjusted based on the loss function's value.

3.2. Evaluation method

This paper adopts the following methods to evaluate the results.

(1) Model evaluation. For the BiLSTM model used in this paper, we use accuracy, sensitivity, specificity, precision, F1 score, confusion matrix to evaluate the classification performance of the model, each index formula is shown in formula (14) to formula (18):

$$Acc = \frac{TP + TN}{TP + FP + TN + FN} \tag{14}$$

$$Se = \frac{TP}{TP + FN} \times 100\% \tag{15}$$

$$Sp = \frac{TN}{TN + FP} \times 100\% \tag{16}$$

$$P = \frac{TP}{TP + FP} \times 100\% \tag{17}$$

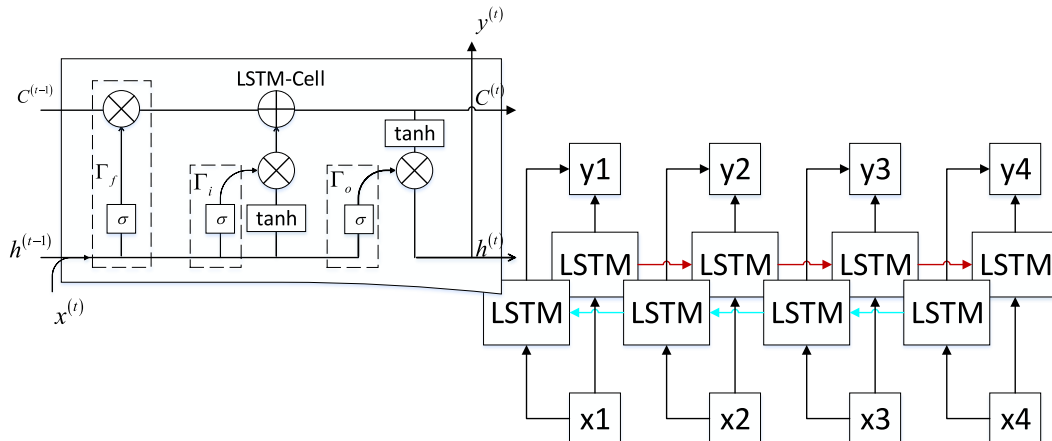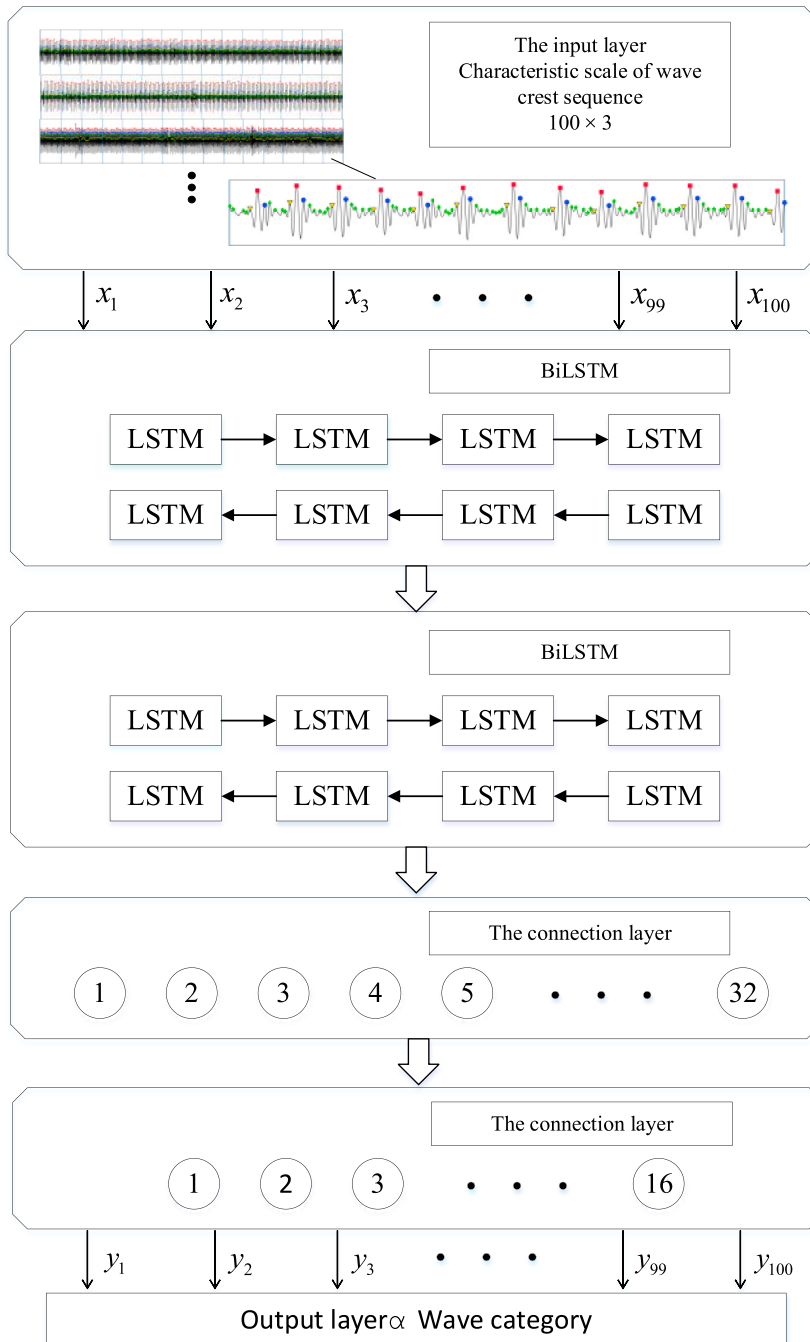$$F1 = \frac{2 \times S_e \times P}{S_e + P} \tag{18}$$

Fig. 4. Structure of BiLSTM.

Fig. 5. Heartbeat detection model framework based on BiLSTM
x1, …,x100:100 × 3 BCG data, where 100 is 100 Ppos, 3are Pa(n), Pd(n) + Td(n) and Pd(n-1) + Td(n-1) y1, …,y100: classification of output results.

Among these metrics, TP stands for true positive, representing the number of samples that are predicted to be positive and are indeed positive. FP stands for false positive, indicating the number of samples that are predicted to be positive but are actually negative. TN stands for true negative, representing the number of samples that are predicted to be negative and are indeed negative. FN stands for false negative, indicating the number of samples that are predicted to be negative but are actually positive.

(2) Heartbeat detection verification. The primary objective of the deep learning model in this study is to precisely locate the J wave, with the accuracy of J wave identification predominantly assessed through the consistency in the number of heartbeats.

Additionally, the reliability of the proposed method is verified by employing metrics such as deviation rate, false positive rate (FPR), false negative rate (FNR), accuracy rate, and recall rate to comprehensively evaluate the heartbeat detection results.

(3) Statistical analysis. Based on the results of heartbeat detection, the characteristic parameters of the BCG signal detection results and the synchronous ECG signal in this study are selected for statistical difference analysis, and the analysis methods are paired sample *t*-test and Pearson correlation coefficient. The ECG heart rate and BCG heart rate of all subjects are analyzed by Bland-Alt method.

4. Experimental results and analysis

4.1. Model evaluation

The dataset contains a total of 1190 feature sequences. In order to avoid the same individual data in the training set and the test set, the dataset is divided into 3:1 ratios. The training set consists of 21 personnel data from all subjects with a sample size of 884, and the data of the remaining 7 subjects is used as a test set with a sample size of 306, and the above information is normalized. In the process of model training, after several debugging and performance analysis, the main training parameters are set as follows: the number of training rounds (epoch) is 100, the sample batch training is adopted, the batch size is set as 50, and the learning rate is 0.01. 20% of the training set data is set as the cross-verification set. In order to speed up the training and improve the training effect, the two-layer BiLSTM sets the random deactivation operation (Dropout) of 0.5 and 0.3, respectively, to reduce overfitting.

The change curve of the loss value and accuracy rate in the training process of the model with the training times is shown in Fig. 6. It can be seen that the model tends to be stable after 60 training times. With the increase of the training rounds, the performance of the model continues to be in a state of slight improvement. Under the premise of training completion, the average code running time of the subjects in the test set is only 0.473s, which show that the method had low latency and could be filled based on the characteristics of sequence length, which could realize real-time detection of heart rate.

Since the purpose of this article is to identify J waves, the setting of labels is essentially two categories: J waves and non-J waves. However, when dividing the labels, it is set to four categories: J wave, H wave, L wave, and other residual waves. There are two reasons for this setting: (1) to balance the quantity of different sample categories. In the prediction task of deep learning, a large gap in the number of different samples will lead to low learning efficiency or even inability to learn. (2) H wave, J wave and L wave are adjacent, and they maintain corresponding sequence information in the continuous BCG wave group, which is conducive to the feature learning of sequence data in BiLSTM. Then, the recognition and classification of J-wave are evaluated. The evaluation process adopts formula (14-18) as the basis for index calculation, and the training model is verified on the test set data. The results are $Acc = 99.67\%$、$Se = 99.14\%$、$Sp = 99.78\%$、$P = 98.89\%$、$F1 = 99.01\%$. The confusion matrix of test set classification. Results are shown in Table 1.

To further validate the effectiveness of the proposed heartbeat detection scheme, it is compared with state-of-the-art methods [31, 32]. While we acknowledge the challenge of accurately comparing with previous studies due to differences in acquisition devices, the structure and parameter settings of the three methods are similar to the network structure proposed in this paper. Specifically, the hidden layer structure setting mode remains consistent with previous studies, with 100 training rounds and a learning rate of 0.01. Each method undergoes testing three times, and the comparison results are presented in Table 2. And the average accuracy of the deep learning model mentioned in this paper can reach 99.33% higher than that of M1 (Time–Frequency Analysis) [34], M2 (ResNet--BiLSTM) [35], M3 (UNet-BiLSTM) [36], M4 (RNN) [31], M5 (LSTM) [24] and M6(GRU) [33], respectively, which reflects the advantages of the proposed model in the J-wave recognition task.

4.2. Analysis of experimental results

In order to accurately reflect the test results into the individual real-time test, the test results of each subject are counted separately. Because BCG signal belongs to the mechanical signal of the heart, itself is not strictly periodic, so the detected BCG cardiac beat position should lag behind the ECG cardiac beat position, and there will be a slight difference between the JJ interval and the RR
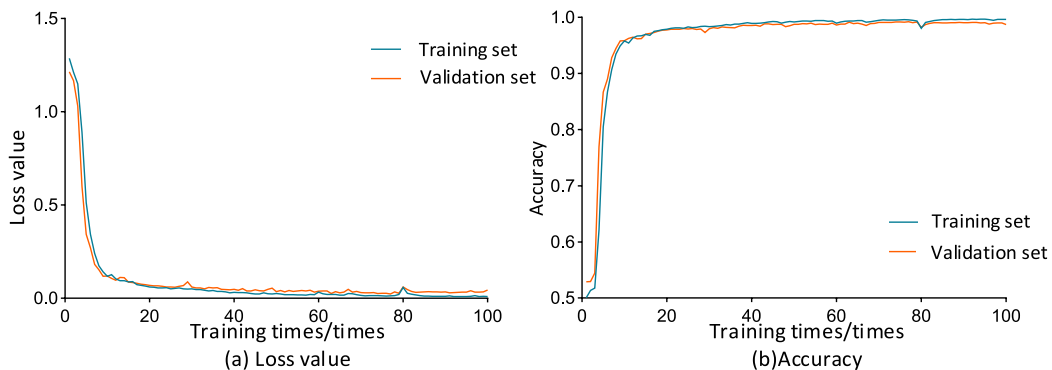

Fig. 6. The curve of loss function and accuracy.

Table 1

J-wave classification confusion matrix of test set.

| The actual category	Predicted class	
	J wave	Not J wave
J wave	5086	44
Not J wave	57	25413

According to various evaluation indexes and Table 1, the model shows a high precision in the classification of J-wave and non-J-wave, with all evaluation indexes reaching about 99%, which reflects a high comprehensive evaluation ability of the model.

Table 2

Comparison of accuracy of different methods.

Case	Accuracy			
	The first time	The second time	The third time	On average
M1	96.22%	96.35%	98.21%	96.93%
M2	98.44%	97.87%	96.34%	97.55%
M3	89.32%	89.32%	89.32%	89.32%
M4	92.52%	91.33%	92.79%	92.21%
M5	93.97%	92.33%	93.32%	93.21%
M6	95.99%	94.98%	96.02%	95.66%
Proposed method	98.99%	99.67%	99.32%	99.33%

interval. The J-wave detection results of one subject are visually represented by three graphical methods. Fig. 7a illustrates the comparison between the Ballistocardiogram (BCG) heartbeat detection results of the subject and the Electrocardiogram (ECG). In the above figure, the red mark is the position of point R of the ECG, which is used as the reference standard of this study; in the following figure, the red mark is the label of point J of BCG, and the blue mark is the recognition result. The comparison results between JJ interval and RR interval are shown in Fig. 7b. From the figure, it's evident that the JJ interval closely aligns with the RR interval, suggesting a notable consistency between the JJ interval and RR interval detected in this paper within a specific error margin. Fig. 7c presents the Bland-Altman plot of JJ interval and RR interval. It's observable that the detection outcomes predominantly fall within the 95% confidence interval, indicating strong agreement between the ECG signal and the BCG signal concerning the cardiogram interval. This finding validates the feasibility of the J-point localization method proposed in this paper.

Table 3 shows the calibration results of the personnel in the test set. Where, P is the accuracy rate, Se is the recall rate, FPR is the
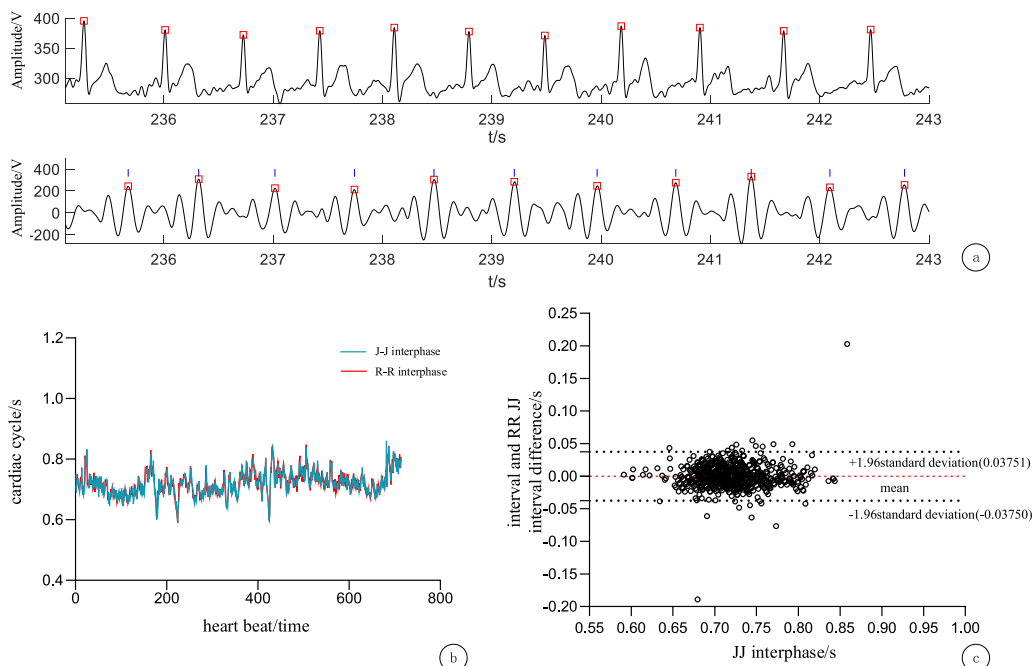

Fig. 7. Comparison between ECG and BCG a. Heartbeat comparison; b. Comparison between JJ interval and RR interval; c. Bland-Altman plot.

Table 3
Heartbeat detection results based on BiLSTM.

No.	heartbeat/time	TP	FNR%	P%	FPR%	E%	Se%
1	609	609	0.16%	99.84%	0.02%	0	99.84%
2	714	714	0	100%	0	0	100%
3	819	812	1.69%	97.48%	0.52%	0.86%	98.31%
4	680	680	0.73%	99.27%	0.15%	0	99.27%
5	946	945	0	99.89%	0.02%	0.11%	100%
6	674	672	3.45%	96.28%	0.82%	0.30%	96.55%
7	702	698	0	99.57%	0.08%	0.57%	100%
Average	735	733	0.85%	98.90%	0.22%	0.27%	99.15%

Table 4
Comparison of statistical parameters of BCG and ECG signal characteristic parameters.

No.	HR_{BCG} /min	HR_{ECG} /min	R value	P value	During the period of the JJ/s	During the period of the RR/s	R value	P value
1	68.81 ± 1.35	68.38 ± 1.88	0.948	0.827	0.877 ± 0.051	0.880 ± 0.036	0.821	0.814
2	71.33 ± 2.73	71.11 ± 2.75	0.945	0.894	0.840 ± 0.032	0.841 ± 0.031	0.923	0.889
3	85.20 ± 2.16	85.11 ± 2.11	0.938	0.723	0.710 ± 0.045	0.706 ± 0.028	0.902	0.663
4	69.88 ± 1.69	69.67 ± 1.58	0.976	0.773	0.861 ± 0.018	0.862 ± 0.015	0.937	0.794
5	67.22 ± 0.86	67.18 ± 0.83	0.985	0.908	0.885 ± 0.068	0.884 ± 0.068	0.966	0.954
6	64.72 ± 1.68	64.30 ± 1.72	0.941	0.806	0.917 ± 0.094	0.922 ± 0.082	0.859	0.716
7	81.18 ± 3.12	80.63 ± 3.14	0.916	0.738	0.718 ± 0.052	0.722 ± 0.043	0.835	0.721
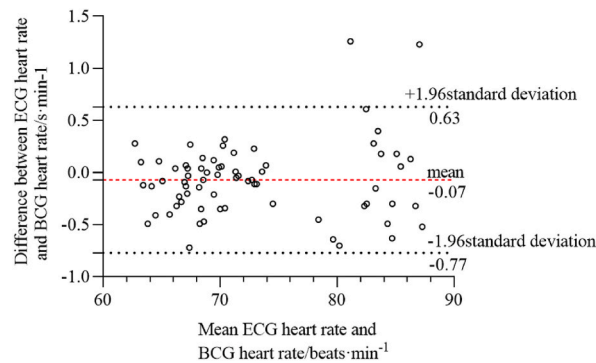
Fig. 8. Bland-Altman plot of heart rate obtained by ECG and BCG.

false positive rate, FNR is the false negative rate, E is the deviation rate of the detection results, TP is the number of heart rate labels in the test set, and JJ is the number of intervals as the detected heartbeat results. It can be seen from Table 2 that the accuracy rate is as high as 99.73%, and the average deviation of all subjects is only 0.27%. This further verifies the accuracy and effectiveness of the proposed method, which can achieve an average false negative rate of less than 1%. Some samples with unsatisfactory results are mainly due to the interference of the collection process or the distortion of BCG signal in the abnormal sleeping position, which make some waveforms irregular and do not conform to the sequence characteristic rule learned by the model. The advantage of deep learning is that the overfitting phenomenon can be weakened by expanding the sample size. When the expanded sample size is sufficient, part of BCG waveforms with special shapes can also be correctly identified. In terms of recall rate and accuracy rate, the identification method in this paper reaches 99.15% and 98.90% respectively, which has high accuracy. According to the above evaluation indicators, this experiment has a higher overall accuracy in the research in the same field, can meet the needs of high-precision heart rate monitoring, and has stronger expansion value.

4.3. Statistical analysis

In the process of heartbeat detection, the average heart rate and heartbeat interval can be carried out on the basis of wave crest recognition. According to the sample T-test and Pearson correlation coefficient statistics, the method proposed in this paper is effective, and the specific calculation indicators are shown in Table 4. The heart rate and JJ interval calculated by BCG signal are not significantly different from the heart rate and RR interval calculated by ECG signal ($P > 0.05$). The Pearson correlation coefficient R values are all in the range of 0.8–1.0, indicating that the BCG signal is strongly correlated with the heart rate and heartbeat interval calculated by the ECG signal. ECG heart rate and BCG heart rate of the subjects are analyzed by Bland-Alt method, and the results are

shown in Fig. 8. The analysis results are basically within the 95% confidence interval. The results above show that BCG signal is feasible to replace ECG signal for heart rate recognition, and the accuracy and feasibility of the proposed method are further verified within the allowable error range.

5. Conclusion

This paper presents a deep learning model tailored for detecting heartbeats from Ballistocardiogram (BCG) signals. Leveraging piezoelectric sensors for vital sign acquisition enables non-contact measurement of BCG signals. We extract morphological features from individual heartbeat intervals, subsequently assembling a dataset based on these features. Real-time heartbeat detection is achieved by quantifying the number of J waves within the input sequence through this model. The decision-making process for heartbeat detection relies on bidirectional Long Short-Term Memory (LSTM), which proves to be effective in locating J-peaks.

To validate our approach, we examine 28 subjects across diverse measurement postures, juxtaposing the detected heartbeat intervals derived from BCG signals against the R–R intervals obtained from ECG signals. The experimental findings illustrate the superiority of our proposed heartbeat detection method over existing benchmarks concerning average accuracy, absolute error, and relative error of beat-to-beat intervals across various measurement postures.

In future research, we envision expanding the dataset and harnessing the advantages of the deep learning algorithm developed in this paper to enable heart rate detection among middle-aged and elderly individuals afflicted with heart-related diseases. This advancement holds promise for the realization of intelligent healthcare solutions, paving the way for enhanced elderly care.

Data availability statement

Data will be made available on request.

CRediT authorship contribution statement

Duyan Geng: Writing – review & editing, Writing – original draft, Conceptualization. **Yue Yin:** Writing – review & editing, Writing – original draft, Conceptualization. **Zhigang Fu:** Conceptualization. **Geng Pang:** Formal analysis, Data curation, Conceptualization. **Guizhi Xu:** Data curation, Conceptualization. **Yan Geng:** Writing – review & editing, Writing – original draft, Conceptualization. **Alan Wang:** Conceptualization.

Declaration of competing interest

The authors declare the following financial interests/personal relationships which may be considered as potential competing interests:Duyan Geng reports financial support was provided by National Natural Science Foundation of China. Guizhi Xu reports financial support was provided by National Key Research and Development Program of China. If there are other authors, they declare that they have no known competing financial interests or personal relationships that could have appeared to influence the work reported in this paper.

Acknowledgment

References

[1] C.V. Anikwe, H.F. Nweke, A.C. Ikegwu, et al., Mobile and wearable sensors for data-driven health monitoring system: state-of-the-art and future prospect, Expert Syst. Appl. 202 (2022) 117362.

[2] D. Kumar, S. Jeuris, J.E. Bardram, et al., Mobile and wearable sensing frameworks for mHealth studies and applications: a systematic review, ACM Trans. Comput. Healthcare 2 (1) (2020) 1–28.

[3] K. Yamamoto, T. Ohtsuki, Non-contact heartbeat detection by heartbeat signal reconstruction based on spectrogram analysis with convolutional LSTM, IEEE Access 8 (2020) 123603–123613.

[4] G. Sannino, G. De Pietro, A deep learning approach for ECG-based heartbeat classification for arrhythmia detection, Future Generat. Comput. Syst. 86 (2018) 446–455.

[5] H.J. Baek, G.S. Chung, K.K. Kim, K.S. Park, A smart health monitoring chair for nonintrusive measurement of biological signals, IEEE Trans. Inf. Technol. Biomed. 16 (1) (2012) 150–158.

[6] C.J. Deepu, Z. Chen, J.T. Teo, S.H. Ng, X. Yang, Y. Lian, A smart cushion for real-time heart rate monitoring, in: Proceedings of the Conference Proceedings: IEEE Biomedical Circuits and Systems Conference (BioCAS), November 2012. Hsinchu, Taiwan.

[7] B.H. Jansen, B.H. Larson, K. Shankar, Monitoring of the ballistocardiogram with the static charge sensitive bed, IEEE (Inst. Electr. Electron. Eng.) Trans. Biomed. Eng. 38 (8) (1991) 748–751.

[8] J.S. Rajput, M. Sharma, Automated detection of hypertension disease using machine learning and signal processing-based methods[M], in: Advanced Computing and Intelligent Technologies: Proceedings of ICACIT 2022, Springer Nature Singapore, Singapore, 2022, pp. 41–53.

[9] J.S. Rajput, M. Sharma, T.S. Kumar, et al., Automated detection of hypertension using continuous wavelet transform and a deep neural network with Ballistocardiography signals, Int. J. Environ. Res. Publ. Health 19 (7) (2022) 4014.

[10] J.S. Rajput, M. Sharma, D. Kumbhani, et al., Automated detection of hypertension using wavelet transform and nonlinear techniques with ballistocardiogram signals, Inform. Med. Unlocked 26 (2021) 100736.

[11] M. Sharma, J.S. Rajput, R.S. Tan, et al., Automated detection of hypertension using physiological signals: a review, Int. J. Environ. Res. Publ. Health 18 (11) (2021) 5838.

[12] J.S. Rajput, M. Sharma, R. San Tan, et al., Automated detection of severity of hypertension ECG signals using an optimal bi-orthogonal wavelet filter bank, Comput. Biol. Med. 123 (2020) 103924.

[13] J.S. Rajput, M. Sharma, U.R. Acharya, Hypertension diagnosis index for discrimination of high-risk hypertension ECG signals using optimal orthogonal wavelet filter bank, Int. J. Environ. Res. Publ. Health 16 (21) (2019) 4068.

[14] I. Starr, F.C. Wood, Twenty-year studies with the ballistocardiograph: the relation between the amplitude of the first record of "healthy" adults and eventual mortality and morbidity from heart disease, Circulation 23 (5) (1961) 714–732.

[15] O.T. Inan, P.F. Migeotte, K.S. Park, et al., Ballistocardiography and seismocardiography: a review of recent advances, IEEE J. Biomed. Health Inf. 19 (4) (2015) 1414–1427.

[16] J.H. Shin, S.H. Hwang, M.H. Chang, et al., Heart rate variability analysis using a ballistocardiogram during Valsalva manoeuvre and post exercise, Physiol. Meas. 32 (8) (2011) 1239.

[17] J.H. Shin, B.H. Choi, Y.G. Lim, et al., Automatic ballistocardiogram (BCG) beat detection using a template matching approach, Annu. Int. Conf. IEEE Eng. Med. Biol. Soc. 2008 (2008) 1144–1146.

[18] C. Will, K. Shi, F. Lurz, R. Weigel, A. Koelpin, Instantaneous heartbeat detection using a cross-correlation based template matching for continuous wave radar systems, in: 2016 IEEE Topical Conference on Wireless Sensors and Sensor Networks, WiSNet, 2016, pp. 31–34, https://doi.org/10.1109/WISNET.2016.7444314.

[19] J. Jin, X. Wang, S. Li, Y. Wu, A Novel Heart Rate Detection Algorithm in Ballistocardiogram Based on Wavelet Transform, 2009 Second International Workshop on Knowledge Discovery and Data Mining, 2009, pp. 76–79, https://doi.org/10.1109/WKDD.2009.98.

[20] Yu Ren, Liu Wen, Zhigang Gao, An improved peak extraction method for heart rate estimation, J. Biomed. Eng. 36 (5) (2019) 834–840.

[21] C. Brüser, K. Stadlthanner, A. Brauers, et al., Applying machine learning to detect individual heart beats in ballistocardiograms, Annu. Int. Conf. IEEE Eng. Med. Biol. Soc. 2010 (2010) 1926–1929.

[22] G. Shen, M.Q. Yang, B.Y. Zhang, Ballistocardiogram-based heart rate variation monitoring using unsupervised learning, Adv. Transdisciplinary Eng. 7 (2018).

[23] R. Zhao, L. Du, Z. Zhao, et al., Accurate estimation of heart and respiration rates based on an optical fiber sensor using adaptive regulations and statistical classifications spectrum analysis, Front. Digital Health 3 (2021).

[24] F. Murat, O. Yildirim, M. Talo, et al., Application of deep learning techniques for heartbeats detection using ECG signals-analysis and review, Comput. Biol. Med. (2020) 120.

[25] O. Faust, A. Shenfield, M. Kareem, et al., Automated detection of atrial fibrillation using long short-term memory network with RR interval signals, Comput. Biol. Med. 102 (2018) 327–335.

[26] Ö. Yildirim, A novel wavelet sequence based on deep bidirectional LSTM network model for ECG signal classification, Comput. Biol. Med. 96 (2018) 189–202.

[27] E. Fotiadou, R.J.G. van Sloun, J.O.E.H. van Laar, et al., A Dilated Inception CNN-LSTM Network for Fetal Heart Rate estimation[J], Physiological Measurement, 2021.

[28] L. Rosales, M. Skubic, D. Heise, M.J. Devaney, M. Schaumburg, Heartbeat detection from a hydraulic bed sensor using a clustering approach, in: Proceedings of the Conference Proceedings: Annual International Conference of the IEEE Engineering in Medicine and Biology Society, September 2012, pp. 2383–2387. San Diego, CA, USA.

[29] A. Graves, Supervised Sequence Labelling with Recurrent Neural Networks, Springer, Berlin, Heidelberg, 2012.

[30] Y. Ho, S. Wookey, The real-world-weight cross-entropy loss function: modeling the costs of mislabeling, IEEE Access 8 (2020) 4806–4813, https://doi.org/10.1109/ACCESS.2019.2962617.

[31] N. Malešević, V. Petrović, M. Belić, et al., Contactless real-time heartbeat detection via 24 GHz continuous-wave Doppler radar using artificial neural networks, Sensors 20 (8) (2020) 2351.

[32] H. Lu, H. Zhang, Z. Lin, N.S. Huat, A novel deep learning based neural network for heartbeat detection in ballistocardiograph, in: Proceedings of the Conference Proceedings: Annual International Conference of the IEEE Engineering in Medicine and Biology Society, July 2018, pp. 2563–2566. Honolulu, HI, USA,.

[33] D. Hai, C. Chen, R. Yi, et al., Heartbeat detection and rate estimation from ballistocardiograms using the gated recurrent unit network, in: Proceedings of the Conference Proceedings: Annual International Conference of the IEEE Engineering in Medicine and Biology Society, Canada, Montreal, QC, July 2020, pp. 451–454.

[34] B. Becerra-Luna, R. Cartas-Rosado, J.C. Sánchez-García, et al., Heart rate variability assessment using time–frequency analysis in hypotensive and non-hypotensive patients in hemodialysis, Appl. Sci. 10 (17) (2020) 6074.

[35] Y. Liu, Y. Lyu, Z. He, et al., ResNet-BiLSTM: a multiscale deep learning model for heartbeat detection using ballistocardiogram signals, J. Healthcare Eng. (2022) 2022.

[36] Y. Mai, Z. Chen, B. Yu, et al., Non-contact heartbeat detection based on ballistocardiogram using UNet and bidirectional long short-term memory, IEEE J. Biomed. Health Inf. 26 (8) (2022) 3720–3730.